

# PCCP

Accepted Manuscript



This is an *Accepted Manuscript*, which has been through the Royal Society of Chemistry peer review process and has been accepted for publication.

*Accepted Manuscripts* are published online shortly after acceptance, before technical editing, formatting and proof reading. Using this free service, authors can make their results available to the community, in citable form, before we publish the edited article. We will replace this *Accepted Manuscript* with the edited and formatted *Advance Article* as soon as it is available.

You can find more information about *Accepted Manuscripts* in the [Information for Authors](#).

Please note that technical editing may introduce minor changes to the text and/or graphics, which may alter content. The journal's standard [Terms & Conditions](#) and the [Ethical guidelines](#) still apply. In no event shall the Royal Society of Chemistry be held responsible for any errors or omissions in this *Accepted Manuscript* or any consequences arising from the use of any information it contains.

# The role of a structure directing agent tetramethylammonium template in the initial steps of silicate oligomerization in aqueous solution

Cite this: DOI: 10.1039/x0xx00000x

Received 00th January 2012,  
Accepted 00th January 2012

DOI: 10.1039/x0xx00000x

www.rsc.org/

Thuat T. Trinh<sup>a\*</sup>, Khanh-Quang Tran,<sup>b</sup> Xue-Qing Zhang,<sup>c</sup> Rutger A. van Santen,<sup>c</sup>  
Evert Jan Meijer<sup>d\*</sup>

The understanding of the formation of silicate oligomers in the initial stage of zeolite synthesis is of fundamental scientific and technological importance. The use of different organic structure directing agents is known to be a key factor in the formation of different silicate species, and the final zeolite structure. Tetramethylammonium (TMA<sup>+</sup>), for example, is indispensable for the formation of the LTA zeolite type. However, the role of a TMA<sup>+</sup> template has not yet been elucidated at molecular level. In this study, ab-initio molecular dynamic simulations were combined with thermodynamic integration to arrive at an understanding of the role of TMA<sup>+</sup> in the formation of various silicate species, ranging from dimer to 4-ring. Free energy profiles show that trimer and 3-ring silicate are less favourable than other oligomers such as linear tetramer, branched tetramer and 4-ring structures. TMA<sup>+</sup> exhibits an important role in controlling the predominant species in solution via its coordination with silicate structures during reaction process. This can explain that formation of D4R.8TMA crystals, as observed in experiment, is controlled by the single 4-ring formation step.

## 1. Introduction

Zeolites are nanoporous aluminosilicate materials widely used in various industrial applications for their catalytic and separation properties<sup>1</sup>. Zeolites are usually prepared from aqueous gel solutions containing different heteroatom sources, inorganic and/or organic cations acting as structure directing agents (SDA), and the mobilizing agents (hydroxyl or fluoride anions). Numerous experimental<sup>2-10</sup> and theoretical<sup>11-24</sup> studies have focused on the nature and structure of the silicate oligomers in solution, as understanding the formation of silicate oligomer in the initial stage is key for zeolite synthesis.<sup>18,25</sup> The elementary steps for Si(OH)<sub>4</sub> oligomerization were extensively studied by computational approaches using a continuum or explicit model of water.<sup>26</sup> The explicit approach has shown that hydrogen bonding network plays an important role in reaction mechanism.<sup>19,27,28</sup> A common pathway of silicate oligomerization in solution is a two-step mechanism with an initial formation of a penta-coordinated intermediate, followed by a water removal step.<sup>19,20,27-30</sup> Computational studies have shown that the presence of a small counter ions such as Li<sup>+</sup>, NH<sub>4</sub><sup>+</sup> and Na<sup>+</sup> has a strong effect on the activation barrier of the first step,<sup>20,27</sup> while the second step seems to be hardly affected by the presence of counter ions.<sup>27,29</sup> Organic cations are known

to be important as structured directing agent, as inferred from various experimental studies.<sup>31-33</sup>

The use of different organic templates such as tetramethylammonium (TMA<sup>+</sup>), tetraethylammonium (TEA<sup>+</sup>) and tetrapropylammonium (TPA<sup>+</sup>) leads to distinct dominant structures.<sup>8,34,35</sup> For example, TMA<sup>+</sup> is necessary for synthesis of LTA zeolite type. In the very first stage of silicate oligomer formation in solution, double 3-ring (D3R) and double 4-ring (D4R) structures were observed.<sup>8,35</sup> With excess of TMA<sup>+</sup> in solution, only crystals of D4R.8TMA<sup>+</sup> are observed while D3R.6TMA<sup>+</sup> has not been detected.<sup>32,33</sup> Caratzoulas *et al.* proposed that the D3R and D4R structures have different stabilities when interacting with 6TMA<sup>+</sup> or 8TMA<sup>+</sup>.<sup>36</sup> To date, computational studies of the effect of organic templates have been limited.<sup>24,31,36,37</sup> A recent ab-initio molecular dynamics study addressed the silicate dimerization mechanism in the presence of TPA<sup>+</sup>.<sup>29</sup> The study showed that the activation barrier of dimerization increases with the presence of TPA<sup>+</sup>, with an analysis of the trajectory revealing a separation between TPA<sup>+</sup> and the silicate dimer during the reaction process. However, a comprehensive picture of the role of TMA<sup>+</sup> in the formation of silicate oligomers is still lacking, in particular on a molecular level.

In this work, ab-initio molecular dynamic (AIMD) simulations were performed to study the formation of silicate oligomers in the presence of TMA<sup>+</sup> in aqueous solution, incorporating the water molecules explicitly. Earlier studies (e.g. Refs 19, 29, 50) have shown that it is crucial to include the effect of thermal motion and the presence of explicit water molecules, when modelling aqueous chemical reactions that involve solvent molecules that strongly bind to the reagents, or actively participate in the reaction mechanism. The overall picture of energy profiles and mechanism could change significantly with dynamic and explicit treatment of solvent<sup>19</sup>.

The free energy profiles of the formation pathways of different silicate oligomers were obtained from the AIMD simulations. The study showed that pathway for 4-ring formation is favourable over that of the 3-ring formation. This trend is in contrast with the system without cation, where 3-ring formation is favourable. More interestingly, during the reaction TMA<sup>+</sup> molecules prefer to form a complex with selected silicate structures (dimer, 4-ring, linear and branched tetramer), giving rise to a lowering of the activation barriers. In contrast, the free energy barriers for the trimer and 3-ring formation are higher, which appears to be correlated to the TMA<sup>+</sup> separating from the silicate structures during the reaction process. This work implies that formation of D3R or D4R can be controlled by the single ring formation step.

## 2. Method

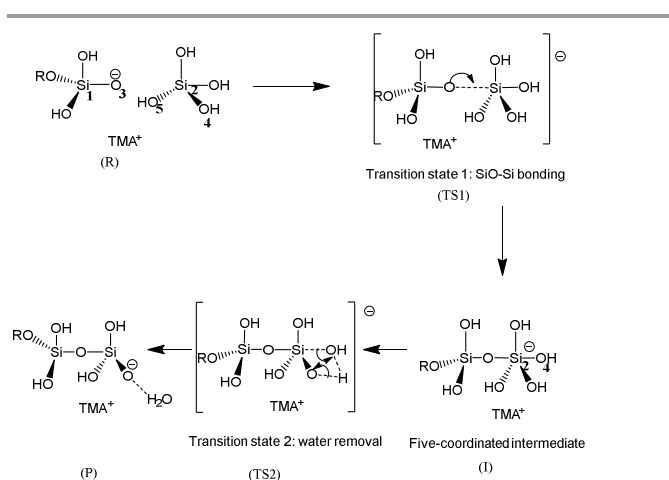
Quickstep<sup>38</sup>, which is part of the CP2K program package<sup>39</sup>, was used to perform AIMD simulations. This package implements a density functional theory (DFT) based Born-Oppenheimer molecular dynamic algorithm, employing a hybrid atom-centered/plane-wave basis set. Goedecker-Teter-Hutter (GTH) pseudopotentials<sup>40, 41</sup> were employed to account for the interactions of the nuclei and core electrons with the valence electrons. The BLYP exchange-correlation functional<sup>42, 43</sup> was used, and complemented with an empirical dispersion correction of Grimme's type<sup>44</sup> to account for the long range van der Waals interactions. The electronic states were expanded using a DZVP-MOLOPT basis set, that provides a double-zeta valence complemented with polarization functions.<sup>45</sup> An energy cut-off of 400 Ry was chosen for the auxiliary plane wave basis set. This computational setup has been successfully employed in earlier computational studies of silicate oligomerization reactions in aqueous solution.<sup>19, 20, 27</sup>

The MD trajectories were calculated with a time step of 0.5 fs. A velocity rescaling thermostat<sup>46</sup> with a time constant of 1000 fs was used to impose a temperature to 350K. The electronic energy was converged to 10<sup>-6</sup> Hartree with the orbital transformation method.<sup>47</sup>

The simulation cell was a periodic orthorhombic box (12x12x25 Å<sup>3</sup>) with a density similar to that of the experimental value of the system under consideration, i.e. around 1g/cm<sup>3</sup>. The initial geometry of the silicate oligomer and TMA<sup>+</sup> was a gas phase optimized structure. This structure was solvated by 132 water molecules, and subsequently a 20 ps trajectory was generated to obtain a equilibrated starting point. The total

number of atoms in system was in the range of 450-460. Reaction pathways were determined by simulating the system for a series of values of a proper reaction coordinate. For each value of the reaction coordinate, the initial configuration was taken from the last configuration of the simulation at the previous value of the reaction coordinate. After 1 ps of equilibration, a 10 ps trajectory was generated to collect data. The total trajectory for the simulation of a reaction pathway, consisting typically of 20 reaction coordinate values, was around 200 ps. This setup allows for a proper sampling of the important dynamical rearrangements, including water reorientation, hydrogen bond breaking and forming, and local translational displacements. This was confirmed by sufficient statistical accuracy of the free energy calculations.<sup>29</sup> The free energy ( $\Delta G$ ) profiles of the oligomerization reactions were obtained by thermodynamic integration using Equation (1), where  $F$  is the calculated constraint force and  $r$  the reaction coordinate. The errors of the constrained force are typically below 10<sup>-5</sup> Hartree/Bohr in 10 ps production run. This approach has been used extensively in earlier studies to calculate free energy barrier reactions in solution.<sup>19, 48, 49</sup>

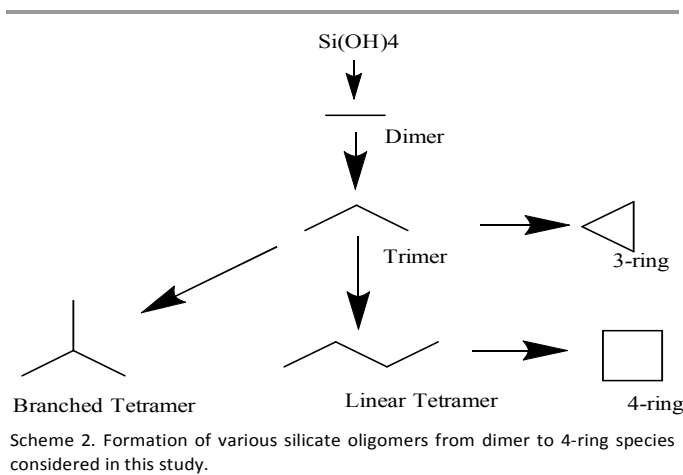
$$\Delta G = -\int_{r_1}^{r_2} \langle F(r) \rangle dr \quad (1)$$



Scheme 1. Schematic representation of the silicate condensation reaction mechanism in a high-pH solution. The reaction coordinate for the first step is taken as the distance between O<sub>3</sub>-Si<sub>2</sub>, and for the second step the Si<sub>2</sub>-O<sub>4</sub> distance.

A common two-step mechanism of silicate oligomerization reaction in aqueous solution is described in Scheme 1.<sup>27</sup> The first step is the formation of a OSi-O bond to form a five-fold coordinated intermediate. The distance between atom O<sub>3</sub> and Si<sub>2</sub> was selected as reaction coordinate, to describe the first step (O<sub>3</sub> atom is the reactive oxygen). The second step is the water removal process, where the distance between Si<sub>2</sub> and O<sub>4</sub> was taken as the reaction coordinate. A similar mechanism for ring closure reaction was proposed.<sup>19,27</sup> We examined 6

oligomerization reactions under basic conditions ( $\text{pH} > 7$ ), ranging from the formation of a dimer up to 4-ring structures (Scheme 2).



### 3. Results and discussion

From the unconstrained MD simulations of the  $\text{TMA}^+$ -silicate systems we obtained radial distribution functions (RDFs). These quantify the water structure, and the solvation of the silicate and the  $\text{TMA}^+$  template in the water network. Fig. 1 shows water-water RDFs for the solvated silicate dimer in the presence of the  $\text{TMA}^+$  cation. The RDFs are very similar to those of pure water. The first peak in the RDF of oxygen-oxygen is located at around  $2.8\text{\AA}$ , which is close to what is observed experimentally<sup>52</sup> and in simulations.<sup>22, 27, 48, 53</sup> This indicates that the water structure is little affected by the presence of the silicate and  $\text{TMA}^+$  solutes. The peaks in the Si-O RDF are well defined, with the second peak at  $3.8\text{\AA}$  describing the first solvation shell of silicate. The solvation of the  $\text{TMA}^+$ , characterized by the N-O RDF is less pronounced, with a first solvation peak at around  $4.5\text{\AA}$ . This observation is consistent with the fact that  $\text{TMA}^+$  is hydrophobic, and matches experimental data of  $\text{TMA}^+$  in water, where the first peak of  $\text{TMA}^+-\text{O}$  RDF was reported at  $4.7\text{\AA}$ .<sup>54</sup>

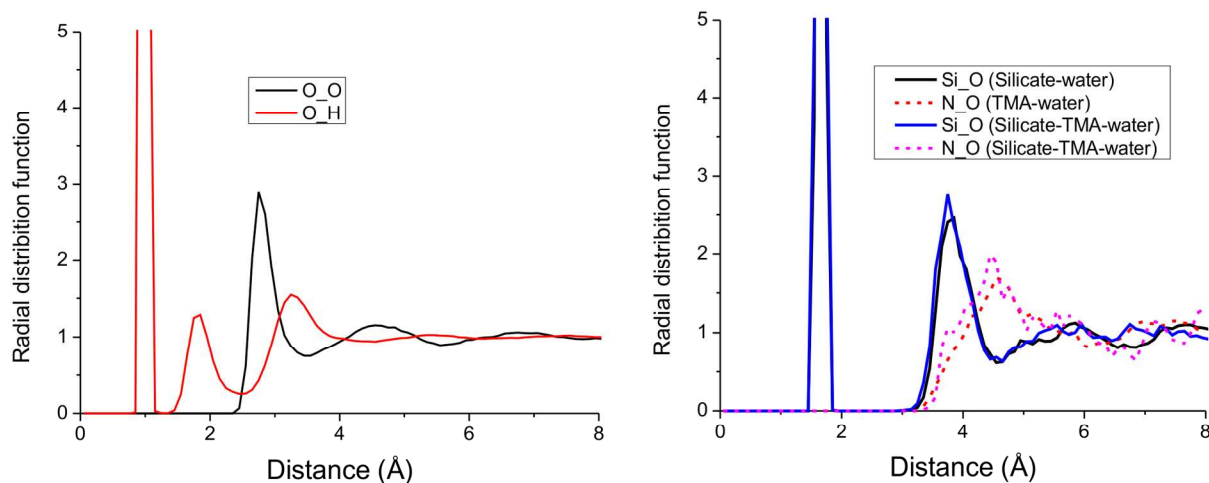


Figure 1. Radial distribution function for O-O and O-H of water (left) and between Si-O, N-O (right)

#### Formation of linear oligomers

In this section we discuss the results obtained for the dimer, trimer, and linear tetramer, respectively. Snapshots of the dimerization reaction are shown in Fig. 2. Overall, the mechanism is similar to that observed for simulations of reactions with different templates<sup>27, 29</sup>. The first step, i.e. the formation of SiO-Si bond, yields a locally stable five-fold coordinated intermediate. Subsequently, a water molecule splits off yielding the dimer species. Earlier studies reported that the presence of an inorganic cation ( $\text{Na}^+$ ,  $\text{Li}^+$  or  $\text{NH}_4^+$ ) has a significant effect on the reaction barrier of the first step and the overall reaction barrier.<sup>27</sup>

Table 1 Total free energy barriers (kJ/mol) obtained by ab-initio MD of silicate oligomerization reaction with presence of TMA<sup>+</sup>. The energies without cation<sup>19, 51</sup> and with the presence of TPA<sup>+</sup>,<sup>29</sup> Na<sup>+</sup>,<sup>27</sup> Li<sup>+</sup>,<sup>20</sup> NH<sub>4</sub><sup>+20</sup> are added for comparison.

Free energy barrier	TMA <sup>+</sup> (this work)	TPA <sup>+</sup>	Na <sup>+</sup>	Li <sup>+</sup>	NH <sub>4</sub> <sup>+</sup>	Without cation
Dimer	78	75	81	98	120	61
Trimer	94	/	75	108	73	53
Linear Tetramer	74	/	/	/	/	/
3-ring	89	/	80	111	82	72
4-ring	80	/	/	/	/	95
Branched Tetramer	72	/	/	80	88	101

Table 1 lists the calculated total reaction free energy barriers, together with calculated data for systems with other cations, as reported in the literature. The accuracy of DFT for the absolute values of the reaction barriers is estimated to be 10-20 kJ/mol. The accuracy for the relative differences in the values of reaction barriers is significantly smaller, and estimated to be ~5 kJ/mol.

The presence of TMA<sup>+</sup> raises the total activation barrier by 17 kJ/mol, when compared to the system without cation<sup>51</sup>. This is consistent with the trend of increasing total activation barrier due to the presence of cations. The origin of the increase could be related to the fact that for the intermediate and transition state silicate structures the negative charge is spatially more distributed than for the reactant silicate structure: this yields an enhanced stabilization of reactant state relative to that of the intermediate and transition state structures. Interestingly, for the dimer, the organic cations TMA<sup>+</sup> and TPA<sup>+</sup> yield comparable barriers, that appears to be lower than those obtained for the systems with inorganic cations. Analysis of the MD trajectories suggests that the reason for a low barrier is that the active oxygen in the first step of reaction (O<sub>3</sub> in scheme 1) has no direct contact with the organic cation.<sup>29</sup> In earlier simulation studies<sup>20, 27, 29</sup> it was demonstrated that, for the first step of the reaction, direct coordination of a cation to the active oxygen gives rise to a higher barrier and a higher free energy of the intermediate. Apparently, the nature of the TMA<sup>+</sup> and TPA<sup>+</sup>, being larger hydrophobic compounds, favours a more distant coordination.

Table 2 lists the calculated free energies, distinguishing the first and second step of the reaction pathway. A complementary, more detailed picture, is provided in Fig. 3 where the calculated free energy profiles are shown.

Table 2. Free energy (kJ/mol) profiles along the silicate formation with the presence of TMA<sup>+</sup> obtained by ab-initio MD.

Free energy	Reactant	TS1	Intermediate	TS2	Product
Dimer	0	71	54	78	29
Trimer	0	72	61	94	26
Linear Tetramer	0	58	44	74	0
3-ring	0	65	54	89	31
4-ring	0	79	67	80	25
Branched Tetramer	0	72	45	72	18

Comparing the overall free energy profiles for formation of linear structures shows that the activation barrier is highest for the trimer. The linear tetramer, which has not been studied in earlier studies, has the lowest total activation barrier among these species. This is due to more stable structures of the transition state 1 and intermediate as shown in Fig. 3. The stability of the linear tetramer appears to be larger than that of the trimer and dimer. This indicates that the rate-limiting step for linear growth of silicate is the formation of the trimer.

The free energy barriers of the second step for the formation of linear silicates are in range of 24-35 kJ/mol. These values, as well as the reactions mechanism, are very similar to those observed in simulations of systems with other cations.<sup>19, 20, 27</sup> The leaving hydroxyl group forms well-defined hydrogen bonds with water molecules. It is protonated either directly by another silicate hydroxyl group, or via a proton transfer chain mediated by one or more water molecules. Representative snapshots of this process are shown in Fig. 4. Still, there appears to be some effect by the presence of a cation, as discussed below.

Comparison of the present results with those obtained for systems with other cations gives the following picture. For the dimerization reaction, similar activation barriers were obtained for the case of TMA<sup>+</sup> and TPA<sup>+</sup>. The relative barrier heights for dimer and trimer formation in the presence of TMA<sup>+</sup> is the reversed of what is observed in a system with a NH<sub>4</sub><sup>+</sup> cation, where dimer formation barrier is substantially higher than that of the trimer formation.<sup>20</sup> In the presence of Na<sup>+</sup> the dimer and trimer barrier are comparable,<sup>27</sup> whereas Li<sup>+</sup> cation appears to have the same effect as TMA<sup>+</sup> on the relative heights of the dimer and trimer formation barrier.<sup>20</sup>

In earlier studies the variation in barrier heights was correlated to the relative position of the cation to the reacting species. In the present study we monitored the relative position of TMA<sup>+</sup> by measuring the distance between the nitrogen atom of TMA<sup>+</sup> and the nearest Si atom of the silicate. The averages of this N-Si distance distribution is plotted against the reaction coordinate and presented in Fig. 5. It is interesting to observe that during dimer and linear tetramer formations, the TMA<sup>+</sup> stays close to the silicate, whereas in the trimerization reaction, it starts departing from the silicate in the initial stage of the water removal step of the reaction. It should be noted that the TMA<sup>+</sup> and silicate were initially located close to each other and a 20

ps equilibration run was performed to get the starting points. Hence, the separation appears to be correlated to the oligomerization reaction. The distance between TMA<sup>+</sup> and the active oxygen follows the shortest distance between TMA<sup>+</sup> and silicate. The active oxygen does never directly coordinated to

hydrophobic TMA<sup>+</sup>, but instead is hydrogen bonded to a water molecule.<sup>29</sup> The electrostatic interaction between this oxygen and TMA<sup>+</sup> induces coordination on a slightly further distance.

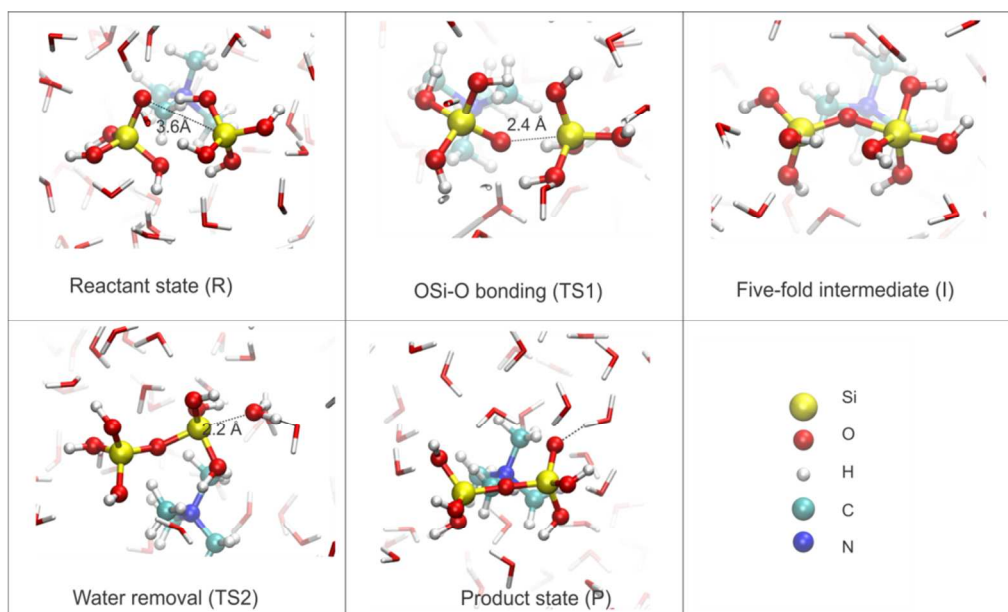


Figure 2. Representative snapshot of dimerization reaction from reactant state to product state following scheme 1. During reaction, TMA<sup>+</sup> stays close to the silicate dimer structure.

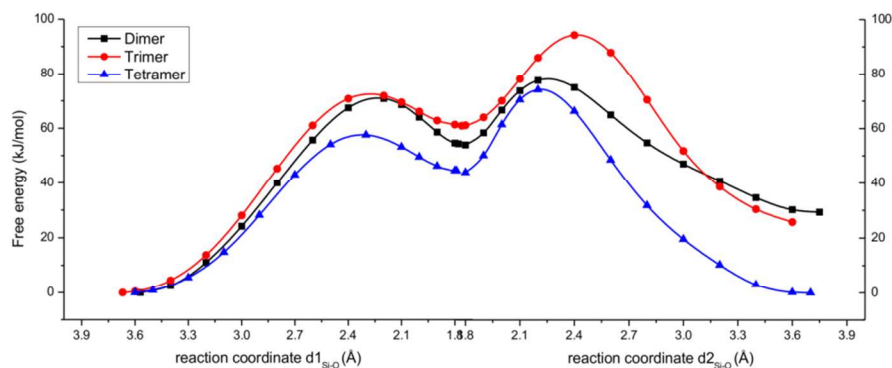


Figure 3. Calculated free energy profile of formation of linear silicate oligomer as functions of reaction coordinate.

The pair separation was due to different hydrogen bond network.<sup>29</sup> Apparently, the binding of TMA<sup>+</sup> to the dimer and linear tetramer helps to reduce the free energy barrier of forming these species, even if it does not actively participate in the water removal reaction. The correlation between the presence of TMA<sup>+</sup> in the first coordination shell of the silicate species and the water removal reaction barrier can be rationalized in view of the fact that this part of the reaction

involves a proton transfer process mediated by the hydrogen bond network around the silicate. A similar pattern has been observed in a system with a NH<sub>4</sub><sup>+</sup> cation present: the water removal step in the trimer formation involved an actively participating nearby cation yielding a relative low barrier, whereas in the dimer formation the NH<sub>4</sub><sup>+</sup> cation was at a larger distance from the leaving water molecule giving rise to a higher barrier.<sup>20</sup>

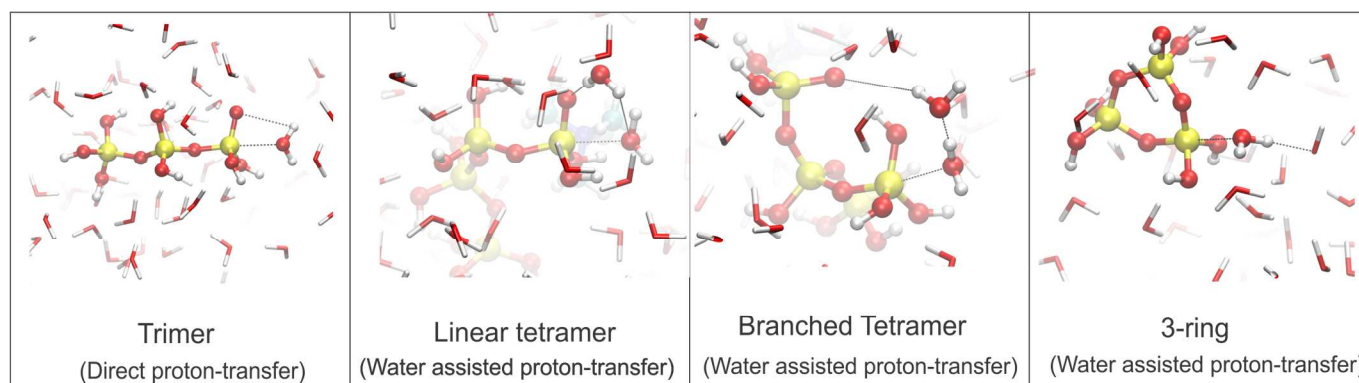


Figure 4. Representative snapshot near the transition state of the second stage of the trimer, linear tetramer, branched tetramer, and 3-ring formation. The mechanism for dimer and 4-ring formations are presented in Fig. 2 and Fig. 6, respectively. During the second stage a water is split off through the release of a hydroxyl with in addition a proton transfer.

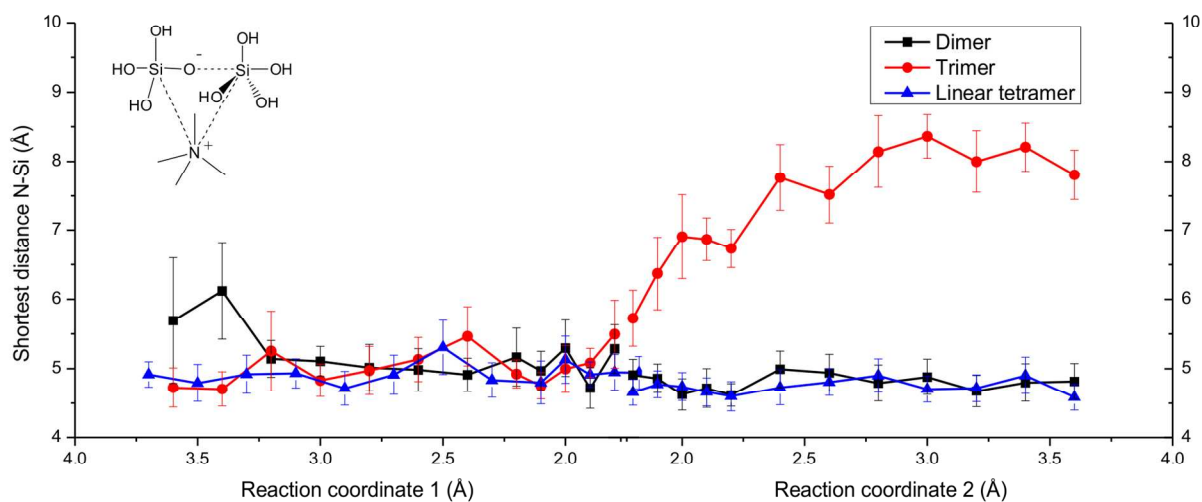


Figure 5. Shortest distance between nitrogen of  $\text{TMA}^+$  and Si of silicate as function of reaction coordinate for linear structure formation. The error bars indicate the width of the measured distance distribution. Only in the case of trimer formation, there is a separation between  $\text{TMA}^+$ -silicate, occurring at the second stage of the reaction.

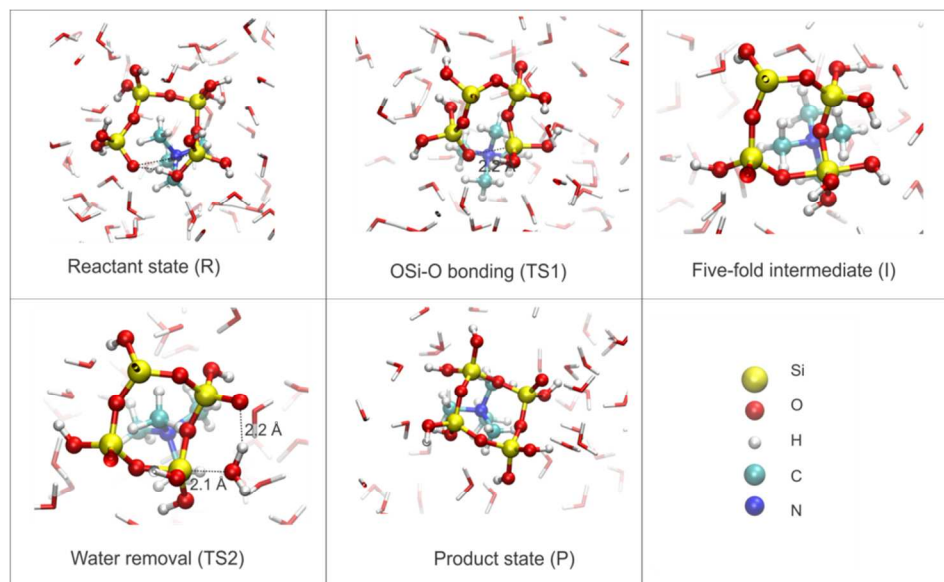


Figure 6. Representative snapshot of 4-ring closure reaction. In the transition state (TS2) of water removal, internal proton transfer to the leaving hydroxyl group. During reaction, TMA<sup>+</sup> stays close to the silicate dimer structure.

### Formation of ring and branched oligomers

The formation of branched or ring structures in the initial stage of silicate formation is a crucial step in zeolite synthesis<sup>28</sup>, following the formation of linear structures. In particular, the formation of the initial 3-ring or 4-ring structures<sup>30</sup> is a deciding factor for the final ring structure of the zeolite. The mechanism of the 3-ring and 4-ring formations from linear oligomers is similar to that seen in the formation of linear structures. Details of this ring closure reaction in the absence of a cation have been presented earlier.<sup>19</sup> Fig. 6 presents snapshots of the calculated reaction pathway for the 4-ring formation, in the presence of TMA<sup>+</sup>. At the first step, the active oxygen atom from one end of the linear tetramer binds to the Si atom at the other end, yielding a ring intermediate. At the second step, water removal occurs yielding the final product. It is interesting that the leaving hydroxyl group is protonated via an internal transfer mechanism, receiving the proton of an adjacent hydroxyl group.<sup>19, 27</sup> This is due to a specific arrangement of hydrogen bond network around the silicate when the water removal takes place.<sup>19</sup>

The free energy profiles of the formation of the 3-ring, 4-ring and branched tetramer are shown in Fig. 7, with the numerical values listed in Table 2. The branched tetramer has the lowest free energy barrier (72 kJ/mol), similar to that for the formation of the linear tetramer (74 kJ/mol). It yields also the most stable product (Table 2). The formation of the 3-ring has a higher

barrier than the 4-ring formation. The low barrier of the second step favours the formation of 4-ring over 3-ring, despite the relative instability of the 4-ring intermediate. This trend is opposite in the system without cation, where formation of the 3-ring has a lower barrier than the 4-ring formation.<sup>19, 51</sup>

Fig. 8 shows the shortest distance between a Si atom of the silicate and the TMA<sup>+</sup> nitrogen as function of the reaction coordinate. The position of TMA<sup>+</sup> is relatively stable during the 4-ring and branched tetramer formation. TMA<sup>+</sup> is positioned near the center of the 4-ring structure (Fig. 6). In the case of 3-ring closure reaction, TMA<sup>+</sup> tends to be dissociated from the silicate during almost the full reaction pathway. This observation is somewhat reminiscent to the case of the linear trimer formation, where TMA<sup>+</sup> dissociates from the trimer at the second step of the reaction. To investigate this further, we performed additional simulations to study the separation between TMA<sup>+</sup> and 3-ring and 4-ring silicate, starting with a configuration with the TMA<sup>+</sup> is in a close contact with 3-ring and 4-ring. During a 10 ps NVT simulation, a separation process was observed in the case of 3-ring, where TMA<sup>+</sup> moves the facial position to the edge of 3-ring. In contrast, TMA<sup>+</sup> remains at the face of 4-ring structures (Fig.9). This observation confirms that TMA<sup>+</sup> does not bind to the face of 3-ring but does in the case of the 4-ring.<sup>36</sup> As both the trimer and 3-ring formation have a relatively high barrier (Table 1), the larger separation of the TMA<sup>+</sup>/silicate pair for these reactions could be

correlated with this. The precise molecular picture requires further investigation.

The calculations show that the formation of a 3-ring facet is suppressed in the presence of  $\text{TMA}^+$ , and that the negatively charge of 3-ring cannot be neutralized to form crystal of D3R with excess of  $\text{TMA}^+$ . In contrast,  $\text{TMA}^+$  appears to show a strong pair with 4-ring during the ring-closure process. The  $\text{TMA}^+$  remains close to the 4-ring facet in solutions and hence, crystalline of D4R and  $8\text{TMA}^+$  can be formed as reported in experimental work.<sup>32, 33</sup>

The observation that reaction free energies are positive in the present computational setup is consistent with previous theoretical reports.<sup>19, 27, 29</sup> The reason is that the overall reaction

produces one extra water molecule yielding an entropically unfavourable rearrangement of the water structure.<sup>19, 27</sup>

The results (Table 1 and Table 2) imply that, in the presence of  $\text{TMA}^+$ , the linear tetramer and branched tetramer are kinetically favourable. The linear tetramer appears to be the most stable species and can subsequently be converted into a 4-ring structure. As our findings suggest that the formation of 4-rings is favoured over 3-rings, we can expect a predominance of D4R structures with  $\text{TMA}^+$  in the initial stage of zeolite synthesis.<sup>8, 35, 55</sup>

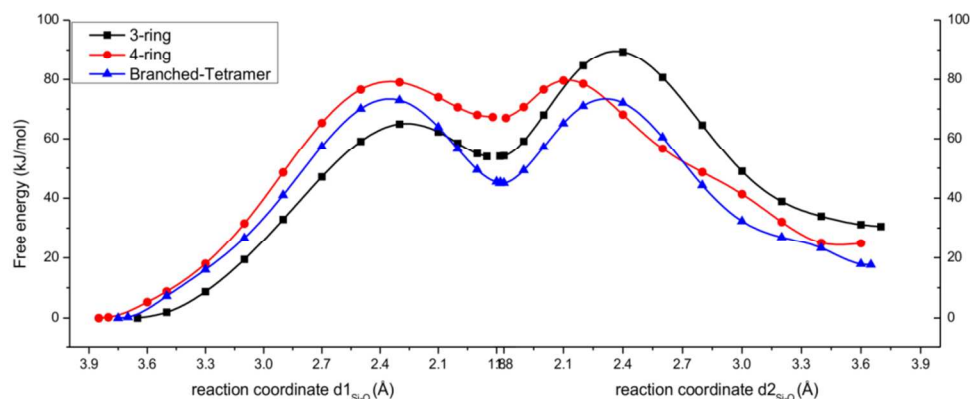


Figure 7. Calculated free energy profile of formation of branched and ring silicate structure as functions of reaction coordinate

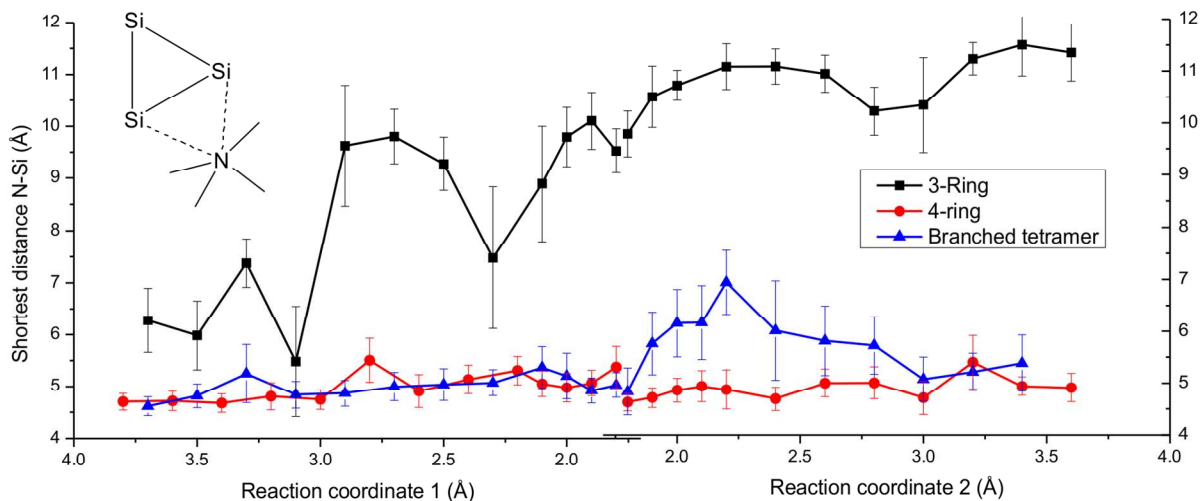


Figure 8. Shortest distance between nitrogen of  $\text{TMA}^+$  and Si of silicate as function of reaction coordinate for ring and branched oligomer formation. The error bars indicate the standard deviation of the distance. Only in the case of 3-ring closure, the separation between  $\text{TMA}^+$ -silicate occurs during the whole reaction process.

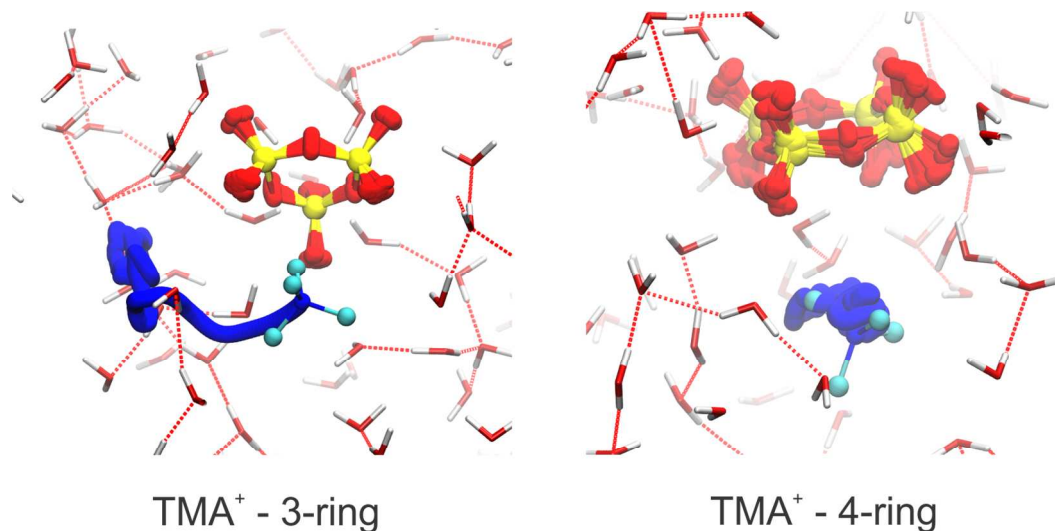


Figure 9. Trajectory presentation shows the movement of TMA<sup>+</sup> in the system with 3-ring and 4-ring during 10 ps simulation. A separation of TMA<sup>+</sup> and 3-ring silicate was observed, while TMA<sup>+</sup> is localized around the face of 4-ring silicate

## Conclusions

The formation of silicate oligomers from dimer to 4-ring in the presence of the organic counterion TMA<sup>+</sup> has been studied using ab-initio molecular dynamic simulations of a model with explicit water molecules. The results show that the presence of TMA<sup>+</sup> increases the free energy barriers of all reactions compared to the case without a counterion, consistent with computational studies of systems with other cations.<sup>20,27,29</sup> The formation of the linear and branched tetramer appears to have lowest free energy barrier. The formation of the trimer appears to be the rate-limiting steps in silicate growth due to the relatively high free energy barrier. In contrast with the case without cation, the presence of TMA<sup>+</sup> favours the formation of 4-ring over 3-rings. TMA<sup>+</sup> coordinates to the silicate oligomers during the formation of the dimer, 4-ring, branched and linear tetramer. In contrast, the TMA<sup>+</sup> and silicate compounds are dissociated for the trimer and 3-ring formation. As the TMA<sup>+</sup> behaves as a hydrophobic solute, the coordination with the silicates is not via a contact ion pair: the electrostatic interaction gives rise to an association on a longer range, yielding a well defined hydrogen bond structure of the water molecules with negatively charged silicate oxygen. This is consistent with results from force field molecular dynamics simulations.<sup>36</sup> The finding that the formation of the tetramers has a lower barrier than the formation of a 3-ring, combined with the observation that linear tetramers are more stable than branched tetramers suggests a dominant presence of 4-ring structures. This may provide a, partly kinetic, explanation why the D4R.8TMA crystalline structures are reportedly observed experimentally, while D3R could not be detected.<sup>32, 33</sup> This

also constitutes a complementary argument, or even an alternative explanation, to the energetic argument that that the D4R structure is thermodynamically stable over the D3R in the presence of TMA<sup>+</sup>.<sup>36</sup> A more definite conclusion requires a further study in order to determine the relative binding free energies between TMA<sup>+</sup> and single ring structures, and to the free energy profiles of the reaction of single to double ring structures.

In conclusion, our results show that TMA<sup>+</sup> plays a directing role during silicate oligomerization. TMA<sup>+</sup> favors the formation of linear, branched and ring tetramer over other structures by a close contact with silicate structures, providing a better insight in the possible formation of the double ring structures in solution.

The present ab-initio molecular dynamics results provide a good basis for further studies. When combined with kinetic Monte Carlo simulation one can arrive at a more comprehensive picture that allows for more accurate comparison with experimental observations.

## Acknowledgements

The authors acknowledge The Research Council of Norway RCN project no. 209337 and The Faculty of Natural Science and Technology, Norwegian University of Science and Technology (NTNU) for financial support. The computational resources were granted by The Norwegian Metacenter for Computational Science (NOTUR) project nn9229k and nn4504k.

## Notes and references

<sup>a</sup> Department of Chemistry, Norwegian University of Science and Technology, Trondheim, Norway.

<sup>b</sup> Department of Energy and Process Engineering, Norwegian University of Science and Technology, Trondheim, Norway.

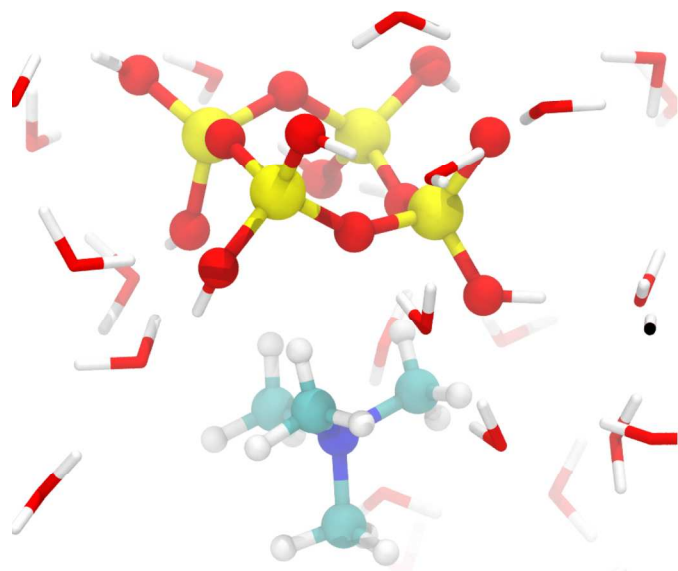
<sup>c</sup> Laboratory of Inorganic Chemistry and Catalysis, ST/SKA, Eindhoven University of Technology, P. O. Box 51 3, 5600 MB Eindhoven, The Netherlands.

<sup>d</sup> Van't Hoff Institute for Molecular Sciences and Amsterdam Center for Multiscale Modeling, University of Amsterdam, Science Park 904, 1098 XH, Amsterdam, The Netherlands.

†email: [thuat.trinh@ntnu.no](mailto:thuat.trinh@ntnu.no) ; [e.j.meijer@uva.nl](mailto:e.j.meijer@uva.nl)

1. C. J. Brinker and G. W. Scherer, *Sol-Gel Science: The Physics and Chemistry of Sol-Gel*, 1990.
2. P. Bussian, F. Sobott, B. Brutschy, W. Schrader and F. Schuth, *Angew. Chem. Int. Ed.*, 2000, 39, 3901.
3. N. Danilina, F. Krumeich, S. A. Castelanelli and J. A. van Bokhoven, *J. Phys. Chem. C*, 2010, 114, 6640-6645.
4. J. Dedecek, S. Sklenak, C. Li, B. Wichterlova, V. Gabova, J. Brus, M. Sierka and J. Sauer, *J. Phys. Chem. C*, 2009, 113, 1447-1458.
5. A. Depla, D. Lesthaeghe, T. S. van Erp, A. Aerts, K. Houthoofd, F. T. Fan, C. Li, V. Van Speybroeck, M. Waroquier, C. E. A. Kirschhock and J. A. Martens, *J. Phys. Chem. C*, 2011, 115, 3562-3571.
6. J. M. Fedeyko, H. Ego-Fox, D. W. Fickel, D. G. Vlachos and R. F. Lobo, *Langmuir*, 2007, 23, 4532-4540.
7. G. J. McIntosh, P. J. Swedlund and T. Sohnel, *Phys. Chem. Chem. Phys.*, 2011, 13, 2314-2322.
8. S. A. Pelster, B. Weimann, B. B. Schaack, W. Schrader and F. Schuth, *Angew. Chem. Int. Ed.*, 2007, 46, 6674-6677.
9. S. Sklenak, J. Dedecek, C. B. Li, B. Wichterlova, V. Gabova, M. Sierka and J. Sauer, *Angew. Chem. Int. Ed.*, 2007, 46, 7286-7289.
10. J. A. Van Bokhoven, T. L. Lee, M. Drakopoulos, C. Lamberti, S. Thiess and J. Zegenhagen, *Nat. Mater.*, 2008, 7, 551-555.
11. J. R. B. Gomes, M. N. D. S. Cordeiro and M. Jorge, *Geochim. Cosmochim. Acta*, 2008, 72, 4421-4439.
12. H. Henschel, A. M. Schneider and M. H. Prosenc, *Chem. Mater.*, 2010, 22, 5105-5111.
13. G. F. Jiao, M. Pu and B. H. Chen, *Struct. Chem.*, 2008, 19, 481-487.
14. X. D. Liu, X. C. Lu, E. J. Meijer, R. C. Wang and H. Q. Zhou, *Geochim. Cosmochim. Acta*, 2010, 74, 510-516.
15. M. J. Mora-Fonz, C. R. A. Catlow and D. W. Lewis, *Angew. Chem. Int. Ed.*, 2005, 44, 3082-3086.
16. M. J. Mora-Fonz, C. R. A. Catlow and D. W. Lewis, *J. Phys. Chem. C*, 2007, 111, 18155-18158.
17. C. L. Schaffer and K. T. Thomson, *J. Phys. Chem. C*, 2008, 112, 12653-12662.
18. T. T. Trinh, A. P. J. Jansen and R. A. van Santen, *J. Phys. Chem. B*, 2006, 110, 23099-23106.
19. T. T. Trinh, A. P. J. Jansen, R. A. van Santen and E. J. Meijer, *J. Phys. Chem. C*, 2009, 113, 2647-2652.
20. T. T. Trinh, A. P. J. Jansen, R. A. van Santen, J. VandeVondele and E. J. Meijer, *ChemPhysChem*, 2009, 10, 1775-1782.
21. C. E. White, J. L. Provis, G. J. Kearley, D. P. Riley and J. S. J. van Deventer, *Dalton Trans.*, 2011, 40, 1348-1355.
22. T. T. Trinh, A. P. J. Jansen, R. A. van Santen and E. J. Meijer, *Phys. Chem. Chem. Phys.*, 2009, 11, 5092-5099.
23. C.-S. Yang, J. M. Mora-Fonz and C. R. A. Catlow, *J. Phys. Chem. C*, 2012, 116, 22121-22128.
24. B. Szyja, P. Vassilev, T. Trinh, R. van Santen and E. Hensen, *Micropor. Mesopor. Mat.*, 2011, 146, 82-87.
25. R. A. Santen and J. W. Niemantsverdriet, *Chemical kinetics and catalysis*, Springer, 1995.
26. Y. Li and J. Yu, *Chem. Rev.*, 2014.
27. A. Pavlova, T. T. Trinh, R. A. van Santen and E. J. Meijer, *Phys. Chem. Chem. Phys.*, 2013, 15, 1123-1129.
28. X. Q. Zhang, T. T. Trinh, R. A. van Santen and A. P. Jansen, *J. Am. Chem. Soc.*, 2011, 133, 6613-6625.
29. T. T. Trinh, X. Rozanska, F. Delbecq and P. Sautet, *Phys. Chem. Chem. Phys.*, 2012, 14, 3369-3380.
30. X. Q. Zhang, T. T. Trinh, R. A. van Santen and A. P. J. Jansen, *J. Phys. Chem. C*, 2011, 115, 9561-9567.
31. S. Caratzoulas, D. G. Vlachos and M. Tsapatsis, *J. Phys. Chem. B*, 2005, 109, 10429-10434.
32. S. D. Kinrade, C. T. G. Knight, D. L. Pole and R. T. Syvitski, *Inorg. Chem.*, 1998, 37, 4272-4277.
33. S. D. Kinrade, C. T. G. Knight, D. L. Pole and R. T. Syvitski, *Inorg. Chem.*, 1998, 37, 4278-4283.
34. B. B. Schaack, W. Schrader and T. Schuth, *Angew. Chem. Int. Ed.*, 2008, 47, 9092-9095.
35. S. A. Pelster, R. Kalamajka, W. Schrader and F. Schuth, *Angew. Chem. Int. Ed.*, 2007, 46, 2299-2302.
36. S. Caratzoulas, D. G. Vlachos and M. Tsapatsis, *J. Am. Chem. Soc.*, 2006, 128, 596-606.
37. S. Caratzoulas and D. G. Vlachos, *J. Phys. Chem. B*, 2008, 112, 7-10.
38. J. VandeVondele, M. Krack, F. Mohamed, M. Parrinello, T. Chassaing and J. Hutter, *Comput. Phys. Commun.*, 2005, 167, 103-128.
39. J. Hutter, M. Iannuzzi, F. Schiffrmann and J. VandeVondele, *Wiley Interdisciplinary Reviews: Computational Molecular Science*, 2014, 4, 15-25.
40. S. Goedecker, M. Teter and J. Hutter, *Phys Rev B Condens Matter*, 1996, 54, 1703-1710.
41. C. Hartwigsen, S. Goedecker and J. Hutter, *Phys. Rev. B*, 1998, 58, 3641.
42. A. D. Becke, *Phys. Rev. A*, 1988, 38, 3098-3100.
43. C. Lee, W. Yang and R. G. Parr, *Phys. Rev. B*, 1988, 37, 785.
44. S. Grimme, *J. Comput. Chem.*, 2006, 27, 1787-1799.
45. J. VandeVondele and J. Hutter, *J. Chem. Phys.*, 2007, 127, 114105.
46. G. Bussi, D. Donadio and M. Parrinello, *J. Chem. Phys.*, 2007, 126, 014101.
47. J. VandeVondele and J. Hutter, *J. Chem. Phys.*, 2003, 118, 4365.
48. T. S. van Erp and E. J. Meijer, *Angew. Chem. Int. Ed.*, 2004, 43, 1659-1662.
49. I. Ivanov and M. L. Klein, *J. Am. Chem. Soc.*, 2002, 124, 13380-13381.
50. C. S. Cundy and P. A. Cox, *Chem. Rev.*, 2003, 103, 663-701.
51. T. T. Trinh, A. P. J. Jansen, R. A. van Santen and E. J. Meijer, *Phys. Chem. Chem. Phys.*, 2009, 11, 5092-5099.
52. A. Soper, *Chem. Phys.*, 2000, 258, 121-137.
53. T. S. van Erp and E. J. Meijer, *Chem. Phys. Lett.*, 2001, 333, 290-296.
54. J. Turner, A. Soper and J. Finney, *J. Chem. Phys.*, 1995, 102, 5438-5443.
55. S. A. Pelster, W. Schrader and F. Schuth, *J. Am. Chem. Soc.*, 2006, 128, 4310-4317.

TOC



TMA. 4-ring silicate